Thermally Induced Microstructure Transitions in a Block Copolymer Ionomer

Xinya Lu,[†,§] W. P. Steckle, Jr.,[†,∥] B. Hsiao,[‡] and R. A. Weiss*,[†]

Polymer Science Program and Department of Chemical Engineering, University of Connecticut, Storrs, Connecticut 06269-3136, and E.I. DuPont de Nemours and Company, Experimental Station, Wilmington, Delaware 19880-0302

Received September 21, 1994; Revised Manuscript Received January 25, 1995[⊗]

ABSTRACT: Microphase transitions of a block copolymer ionomer based on lightly sulfonated poly(styrene-*b*-(*ran*-ethylene-*co*-butylene)-*b*-styrene) (SSEBS) were studied as a function of temperature by time-resolved small-angle X-ray scattering (SAXS). An ionic aggregate dissociation temperature, T_d, was observed for free acid and zinc salt derivatives of SSEBS. This represents the first time that an order–disorder transition has been observed for an ionomer, and it is attributed to a destabilization of the ionic microphase separation by the tendency of the blocks to mix at elevated temperatures. At relatively low sulfonation level (3 mol % of the styrene blocks), the order–disorder transition (ODT) of the block microstructure of Zn-SSEBS coincided with T_d. At intermediate sulfonation levels (8–12 mol %), dissociation of the ionic aggregates was followed by a mesophase–mesophase transition of the block microstructure where the texture changed from ellipsoidal to lamellar. For those materials, no ODT was observed below 300 °C. For the highest sulfonation level (18 mol %), an equilibrium microstructure was difficult to obtain because of the high melt viscosity. No evidence of the ODT was observed below the degradation temperature of the polymer. No microstructure transitions were observed for alkali metal salts due to much more robust ion–dipole interactions in those ionomers.

Introduction

The physical and mechanical properties of multiphase polymer systems are strongly dependent on their morphology and microphase structure. Block copolymers and ionomers are two classes of microphase-separated systems that have been extensively studied during the past few decades.[1–4] Block copolymers exhibit a variety of ordered microphases with a characteristic size scale ~10–100 nm. Microphase separation in block copolymers is due to thermodynamic immiscibility between the component blocks; macrophase separation is prevented by covalent attachment of the two or more block segments. The specific texture of the microstructure depends on composition and the intensity of the driving force for phase separation, i.e., the repulsive interactions between the chemical substituents. The latter parameter depends on the particular chemical species used, the polymer molecular weight, and temperature.

Statistical thermodynamic theories predict the microphase structure of block copolymers,[5–10] and mean-field theories of microphase separation[11,12] predict not only the order–disorder transition but also various mesophase transitions, i.e., transformation from one ordered microphase to another with a different texture. Order–disorder transitions have been observed experimentally for various block copolymers,[13–16] but mesophase transitions have only been reported recently for a few systems.[17–19]

The microstructure of ionomers is less ordered than that for block copolymers, and the characteristic dimensions associated with the microphase separation are at least an order of magnitude smaller, ~2–4 nm. For ionomers, microphase separation is promoted by strong attractive interactions between ions and dipoles.[20–23] Aggregation of the ionic species depends on the dielectric constant of the matrix polymer and the chemistry of the anion and the cation, but the texture of the microstructure is relatively insensitive to the ionic group concentration. A number of models[24–26] for the microstructure of ionomers have been proposed during the past 20 years, but despite extensive experimental work, no definitive confirmation of any single model has emerged. Similarly, although ionic aggregation in ionomers is thought to be thermally reversible,[27] a critical temperature for dissociation of the ionic aggregates, i.e., an order–disorder transition, has not been observed experimentally for either random ionomers[28,29] or telechelic ionomers.[30]

Several research groups have recently consolidated the characteristics of the two different types of microphase-separated polymers into a single material by preparing block copolymer ionomers,[31–37] wherein one of the blocks of a block copolymer contains bonded salt groups. Block copolymer ionomers formed by lightly sulfonating poly(styrene-*b*-(*ran*-ethylene-*co*-butylene)-*b*-styrene) (SEBS) possess a unique morphology that exhibits two different levels of microphase separation, one due to self-assembly of the block structure and another due to ionic aggregation within the microdomains formed by the ionomer blocks.[35] One might expect aggregation of the ionic groups within the ionomeric block to suppress self-assembly of the block microdomains or, conversely, that the restricted geometry imposed by the size of the ordered block microstructure inhibit ionic aggregation. As a result, both the thermodynamics and kinetics of the block and the ionic microphase separation may exhibit notable differences from either the unmodified block copolymer or the corresponding homopolymer ionomer. Order–disorder and mesophase transitions may be perturbed by the combination of the effects of the block microdomains and the ionic aggregates. On the one hand, the order–disorder transition of the block microstructure may increase because of the increased immiscibility between

† University of Connecticut.
‡ E.I. DuPont de Nemours and Co.
§ Current address: Corporate Research Center, International Paper Co., Long Meadow Rd., Tuxedo, NY 10987.
∥ Current address: Materials Science & Technology Division, Los Alamos National Laboratory, Los Alamos, NM 87544.
⊗ Abstract published in *Advance ACS Abstracts,* March 1, 1995.

0024-9297/95/2228-2831$09.00/0 © 1995 American Chemical Society

the ionomeric and neutral blocks. On the other hand, the order–disorder transition of the ionic aggregates may decrease because the driving force for block mixing at elevated temperature might also destabilize the ionic aggregation within the microdomains.

The effects of sulfonation level, the choice of the counterion and sample history on ionic aggregation, and the block microstructure in sulfonated poly(styrene-*b*-(*ran*-ethylene-*co*-butylene)-*b*-styrene) block copolymer ionomers (SSEBS) have been previously reported.[36,37] This paper addresses the subject of thermally-induced microphase transitions in these materials. Time-resolved small-angle X-ray scattering (SAXS) was used to investigate real-time structural evolution of the block microstructure and the ionic aggregates during dynamic heating experiments.

Experimental Section

Materials. The starting SEBS polymer was a hydrogenated triblock copolymer of styrene and butadiene, Kraton 1652, from Shell Development Co. After hydrogenation, the midblock is essentially a random copolymer of ethylene and butylene. The number-average molecular weight, M_n, of the copolymer was 50 000, and the composition was 29.8 wt % styrene. Sulfonated SEBS block copolymer ionomers, SSEBS, were prepared by sulfonating the SEBS with acetyl sulfate in 1,2-dichloroethane at 50 °C.[33] The sulfonation level of the polymer was determined by titration of SSEBS solutions in a mixed solvent of toluene/methanol (90/10, v/v) to a phenolphthalein end point. Na^+, Cs^+, and Zn^{2+} salts of SSEBS were prepared by neutralizing the free acid derivatives (H-SSEBS) in a toluene/methanol mixed solvent with the appropriate alkali hydroxide or zinc acetate dihydrate, respectively. The nomenclature used for the samples is *x.yM*-SSEBS, where *x.y* is the sulfonation level in mole percent of the styrenic block and M denotes the cation (=Na, Cs, or Zn).

Films for SAXS measurements were prepared by solution-casting and by compression-molding. The compression-molding conditions depended on the cation used and the sulfonation level, varying from 150 °C for 2 min for SEBS to 250 °C for 10 min for 12Na-SSEBS. Cast films were prepared from toluene/dimethylformamide (DMF) mixtures varying from 2 to 10% (by volume) DMF, depending on the sulfonation level of the polymer. The solvent was evaporated in air, and final drying was done under vacuum for 2 days at 50 °C. The films were annealed for 2 h at 120 °C prior to the SAXS experiments.

SAXS Measurements. SAXS was performed at the Stanford Synchrotron Radiation Laboratory (SSRL) using beamline I-4 and at the National Synchrotron Light Source (NSLS) at Brookhaven National Laboratories using a modified Kratky SAXS camera on beamline X3A2. The SAXS instruments are described elsewhere.[38,39]

At SSRL, the beam decay and the sample absorption coefficient were monitored by using two detectors placed in the optical path immediately before and after the specimen. The wavelength, λ, of the incident beam was 0.143 nm, and the sample was encapsulated in an aluminum sample cell that was fashioned from a conventional DSC pan. A Mettler FP82 hot stage was used to control the temperature. Two different sample-to-detector distances (SDD) were used to provide a range of the scattering vector, $q = 4\pi(\sin\theta)/\lambda$ where 2θ is the scattering angle, of either 0.06–1.2 nm^{-1} for measuring the block microphase structure or 0.5–5 nm^{-1} for studying the ionic aggregates. All data were corrected for dark current, detector heterogeneity, parasitic and background scattering, and sample absorption.

At NSLS, λ = 0.154 nm, and ionization chambers were placed before and after the sample to determine the decay of the incident beam and the sample absorption coefficient. A Braun position-sensitive detector was used. The sample was placed in a dual-cell high-temperature hot stage for the heating experiments. The SDD was varied to produce a q-range of 0.08–6.3 nm^{-1}.

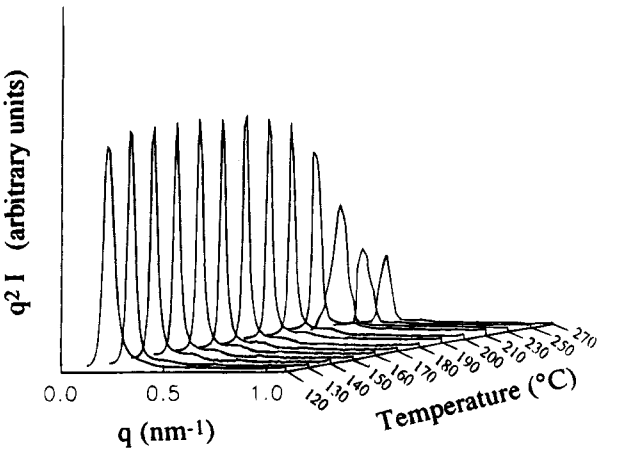

Figure 1. Temperature-resolved SAXS profiles for the block microstructure of compression-molded SEBS obtained while heating from 50 to 250 °C.

Results and Discussion

Effect of Temperature on Block Microstructure. Figures 1 and 2 show Lorentz-corrected SAXS profiles at selected temperatures obtained while heating compression-molded films (CM) of SEBS and 12H-SSEBS from 50 to 270 °C using a heating rate of 10 °C/min. At the lower temperatures, for both materials only a single broad SAXS peak is observed. Transmission electron microscopy of these same samples revealed a block microstructure of ellipsoidal domains, though the phase boundaries were much more diffuse for the ionomer.[35] Although the block microstructures of the as-molded samples of 12H-SSEBS(CM) and SEBS(CM) were similar, the temperature dependences of their scattering patterns were notably different. Above 180 °C, the SAXS intensity of the parent block copolymer (SEBS) began to decrease slightly with increasing temperature due to increased mixing of the component blocks, and an order–disorder transition (ODT) occurred at ca. 220 °C. The ODT is evident from the large decrease in the scattering intensity. The peak does not disappear, because of the correlation between the different blocks even in the disordered state.

For the block copolymer ionomer, increasing temperature notably increased the SAXS intensity, and a second-order maximum was also observed at ca. 175 °C; see Figure 2. That result indicates that annealing 12H-SSEBS at elevated temperatures promoted microphase separation of the block structure and improved the order of the microstructure, in contrast to the unmodified SEBS where mixing of the phases occurred.

The SAXS pattern of 12H-SSEBS in Figure 2 may be divided into three regions: (1) $T < T_g$ of the sulfonated polystyrene block (~90 °C), (2) 90 °C < T < 175 °C, and (3) T > 175 °C. Below the T_g of the sulfonated polystyrene block, only a single SAXS peak was observed, and the intensity of the peak increased with increasing temperature. The increased scattering intensity may arise from either increased phase separation or electron density contrast between the two phases. Below 90 °C, the SPS phase is a glass, and the low molecular mobility makes changes in the volume fractions of the two phases difficult to occur. The electron density contrast between the glassy SPS phase and the EB-rubber phase, however, will increase with increasing temperature as a consequence of the larger thermal expansion coefficient of the rubber.

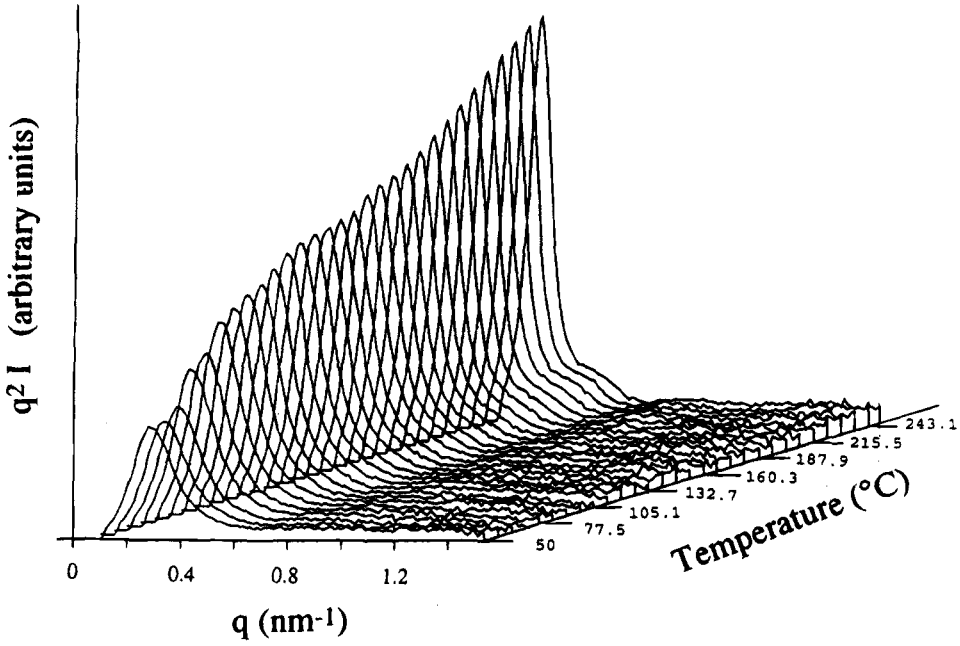

Figure 2. Temperature-resolved SAXS profiles for the block microstructure of compression-molded 12H-SSEBS obtained while heating from 50 to 250 °C.

In region 2, between 90 and 175 °C, the SAXS intensity continued to increase with increasing temperature, but at a slower rate than in region 1. This increase in scattering is also due to differences in the thermal expansion coefficients of the two phases, but the difference is smaller above the T_g of the SPS block.

In region 3, above 175 °C, the intensity of the strong first-order peak increased, the peak sharpened, and a second-order maximum became apparent at a scattering vector of twice that of the first-order peak. The latter feature is characteristic of a lamellar microstructure, which indicates that a mesophase-to-mesophase transition of the block microstructure from ellipsoidal to lamellar occurred at ca. 175 °C.

For block copolymer ionomers, mesophase or order–disorder transitions of the block microstructure cannot occur below the dissociation temperature of the ionic aggregates, which depends on the strength of the ionic interactions and the chain elastic forces that resist ionic association. The temperatures for block mesophase transitions are expected to increase as the strength of the ionic associations increases. In general, the hydrogen bonding in the free acid derivatives is less temperature-resistant than the ion–dipole interactions in metal-neutralized ionomers. As a result, the mesophase transition observed for 12H-SSEBS, ~175 °C, was relatively low compared to that observed for the metal salts. For example, no mesophase transition was observed for 12Zn-SSEBS, though it was observed for block copolymer ionomers with lower sulfonation levels. This will be discussed further later in this paper.

For a two-phase system, the scattering invariant, Q, provides a measure of the extent of phase separation. Q is independent of the microphase texture and may be calculated by the following equation:[39]

$$Q = \frac{1}{2\pi^2 I_e}\int_0^\infty q^2 I(q)\,dq \qquad (1)$$

where I_e is the Thomson scattering constant for an electron. For an ideal two-phase system with sharp phase boundaries, the scattering invariant is

$$Q_0 = \phi_1\phi_2 V(\varrho_1 - \varrho_2)^2 \qquad (2)$$

and the temperature dependence of Q_0 is

$$\frac{Q_0(T)}{Q_0(T_r)} = 1 + (T - T_r)\left[(\alpha_1 - \alpha_2)(\phi_2 - \phi_1) + \frac{2(\alpha_2\varrho_2 - \alpha_1\varrho_1)}{(\varrho_1 - \varrho_2)}\right] \qquad (3)$$

where T_r is a reference temperture and α_i, ϕ_i, and ϱ_i ($i = 1, 2$) are the thermal expansion coefficient, the volume fraction, and electron density of each phase. The reference temperature was arbitrarily defined as 50 °C so that $Q_0(T_r) \equiv Q_0(50)$. The values of α, ϕ, and ϱ used for the SPS and EB phases for the 12M-SSEBS block copolymer ionomers are listed in Table 1.

$Q(T)/Q(50)$ calculated from the SAXS data for 12H-SSEBS in Figure 2 are plotted against temperature in Figure 3. The values for an ideal two-phase system, $Q_0(T)/Q_0(50)$, calculated from eq 3 are also plotted for comparison. Although the quantitative agreement is poor, the trends in the slopes of the two curves below and above T_g of the b-SPS phase are similar. That result supports the premise that the temperature dependence of the observed scattering intensity was due to thermal expansion effects and not changes in the extent of phase separation or composition of the phases. The quantitative discrepancy between $Q_0(T)/Q_0(50)$ and $Q(T)/Q(50)$ is probably due to a nonideal microstructure and uncertainty in the values of the phase volumes and compositions. Most likely there was a diffuse interphase boundary, which has been observed by transmission electron microscopy.[34] In contrast to the SAXS patterns in Figure 1, the invariant exhibited no clear transition at 175 °C, which also bolsters the conclusion that the change in the SAXS pattern at 175 °C corresponded to a transition of the microstructure texture, i.e., a mesophase-to-mesophase transition, rather than a change in the extent of phase separation.

Figure 4 shows the SAXS profiles of 12Na-SSEBS-(CM) as a function of temperature. In contrast to the

Table 1. Values of α_i, ϕ_i, and ϱ_i Used To Calculate $Q(T)$ for *x,yM*-SSEBS

sample	α_g(SPS) $\times 10^4$	α_l(SPS) $\times 10^4$	α_l(EB) $\times 10^4$	ϱ_{EB} (e·mol/cm^3)	ϱ_{SPS} (e·mol/cm^3)	ϕ_{SPS}
12H-SSEBS	1.67	4.23	6.38	0.484	0.583	0.262
12Na-SSEBS	1.67	4.23	6.38	0.484	0.597	0.265
12Zn-SSEBS	1.67	4.23	6.38	0.484	0.622	0.268

behavior of the acid derivative, a single broad maximum was observed over the entire temperature range, and the peak intensity increased monotonically with increasing temperature. The broadening of the scattering peak for the Na salt derivative compared with the scattering peaks for the unmodified block copolymer and the acid derivative of 12-SSEBS (cf. Figures 1, 2, and 4) was due to microphase separation of an ion-rich phase within the *b*-SPS microphase. Ionic aggregation broadens the scattering peak from the block microstructure in two ways: (1) the ionic aggregates create additional electron density fluctuations within the *b*-SPS phase and (2) intermolecular ionic interactions impede the block microphase separation. Those effects produce a more diffuse interphase boundary and, perhaps, a broader distribution of phase sizes. The absence of any evidence of a mesophase transition in Figure 4 is a consequence of the persistence of the ionic aggregates to at least 250 °C in 12Na-SSEBS(CM).

Figure 5 shows the effect of cation on $Q(T)/Q(50)$ for the acid derivative and the sodium and zinc salts of 12M-SSEBS(CM). A change in the slope of $Q(T)$ vs T at the T_g of the *b*-SPS was much more pronounced for the acid derivative than for either salt. The slope decreased slightly at ca. 120 °C for the zinc salt, but the slope remained relatively constant for the sodium salt over the temperature range studied. The higher temperature for the change in slope for the zinc salt than for the acid derivative reflects the higher $(T_g)_{b\text{-ZnSPS}}$ for the salt and was consistent with the value measured by dynamic mechanical thermal analysis.[35] At any given temperature, the vlaue of $Q(T)/Q(50)$ decreased for the three block copolymer ionomers in the order of $H^+ > Zn^{2+} > Na^+$. The slopes of the $Q(T)/Q(50)$ vs T curves for the different 12M-SSEBS(CM) samples were similar above $(T_g)_{b\text{-SPS}}$, but below $(T_g)_{b\text{-SPS}}$ the slopes decreased in the same relative order as the invariant ratio. The decreasing order of the sub-T_g slope and $Q(T)/Q(50)$ corresponds to the increasing strength of the ionic associations in sulfonated polystyrene ionomers.[29] That is, the changes in the invariant due to thermal expansion of the sample decreased as the strength of the ionic interactions increased in the order of $H^+ > Zn^{2+} > Na^+$.

The block microstructure of the block copolymer ionomers is also sensitive to the procedure used to prepare the sample.[36] For example, a lamellar microstructure was obtained for solution-cast 12Zn-SSEBS, as evident from the 2:1 ratio for q of the first- and second-order peaks in the SAXS patterns in Figure 6. Figure 6 also shows the temperature dependence of the SAXS profile of this sample. $Q(T)/Q(50)$ is plotted against temperature in Figure 7. Two changes in the slope occur at ca. 120 and 210 °C. The lower temperature transition corresponds to $(T_g)_{b\text{-ZnSPS}}$ and the higher temperature transition corresponds to the dissociation of the ionic aggregates.

Values of $Q(T)/Q(50)$ for a solution-cast film and a compression-molded sample of 12Zn-SSEBS are compared in Figure 7. The changes in the invariant with

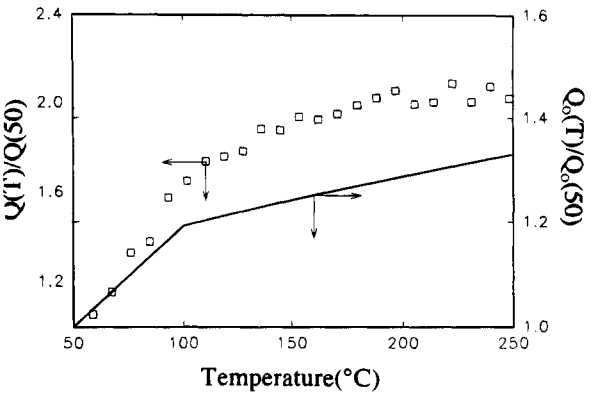

Figure 3. Comparison of experimental $Q(T)/Q(50)$ (points) and predicted $Q_0(T)/Q_0(50)$ (solid line) as a function of temperature for 12H-SSEBS.

increasing temperature were greater for the compression-molded sample, though in both sets of data changes in slope occurred at similar temperatures. That result seems reasonable, because even though the sample preparation influenced the block microstructure and the extent of microphase separation, the glass transition temperature of the *b*-ZnSPS and the ionic dissociation temperature should be relatively insensitive to the block texture. The larger changes of $Q(T)/Q(50)$ for the compression-molded sample may reflect either greater changes in thermal expansion due to poorer development of the block microstructure or may be due to improved development of the microstructure as a result of thermal annealing. Compression molding is unlikely to result in a well-developed order of the morphology because of the hinderance to the formation of the block microstructure of the ionic aggregates, which act as physical cross-links. This is demonstrated by the increased microstructure order for the solution-cast sample, which had a much lower viscosity during the development of the morphology.

Effect of Temperature on Ionic Aggregation. The effect of temperature on the ionic aggregation in ionomers has been studied for SPS ionomers,[28,29] poly(ethylene-*co*-methacrylic acid) ionomers,[28] and telechelic ionomers.[30] In each of those systems, the ionic aggregates were thermally stable, and no dissociation of the aggregates, as predicted by Eisenberg,[27] was observed before the polymers degraded. As discussed earlier, dissociation of the ionic, or in the case of 12H-SSEBS the hydrogen-bonded, aggregates must precede the advent of a mesophase transition in the block copolymer ionomers. The lowering of the ionic dissociation temperature observed in these studies probably results from destabilization of the ionic aggregates by the elastic forces of the polymer chains bonded to the ionic groups and by the forces arising from a tendency for the blocks to mix that also destabilize the ionic aggregation within the *b*-SPS microdomains. Like the elastic force, the additional force due to the block copolymer microstructure becomes more important at elevated temperature. As a result, the net force opposing the aggregate structure exceeds the associative forces at a lower temperature for the block copolymer ionomer than in the corresponding homopolymer ionomer.

SAXS data, normalized by the sample absorption and the beam intensity, for the ionic microstructure of 8.7Zn-SSEBS(CM) obtained while heating the sample from 90 to 250 °C are given in Figure 8. The scattering pattern below 90 °C featured a single, broad peak at $q \sim 1.42$

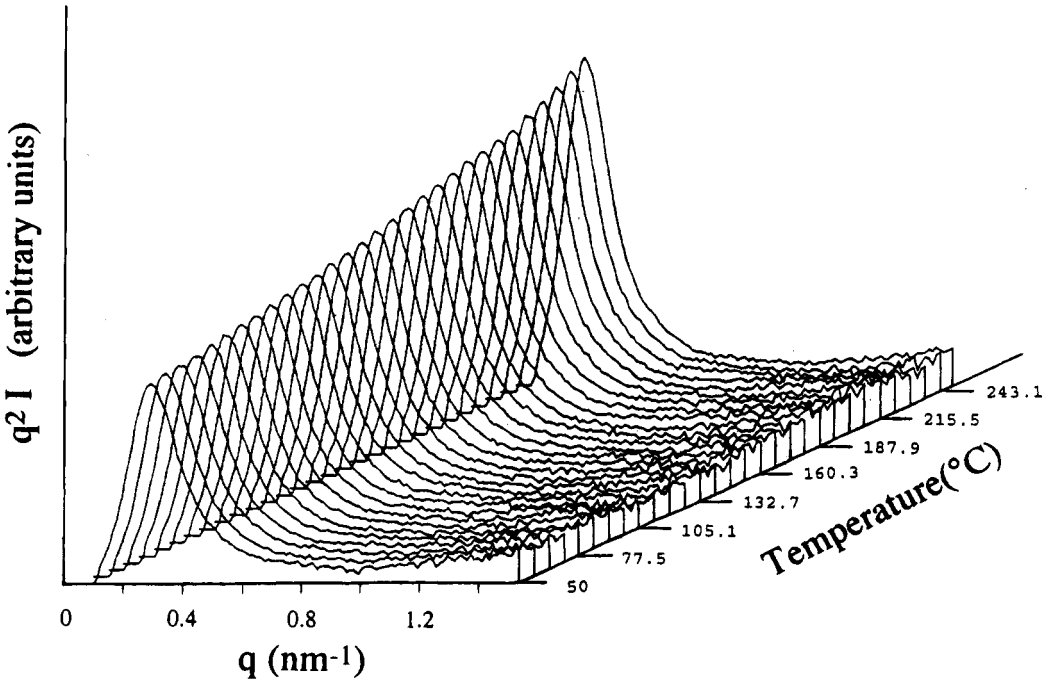

Figure 4. Temperature-resolved SAXS profiles for the block microstructure of compression-molded 12Na-SSEBS obtained while heating from 50 to 250 °C.

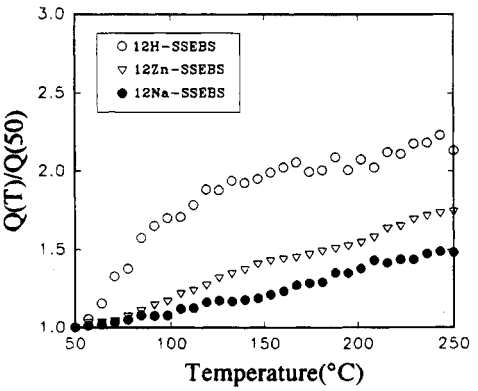

Figure 5. Effects of cation on experimental values of $Q(T)/Q(50)$ for 12M-SSEBS.

nm^{-1}, which is consistent with the classic *ionomer peak* observed for most ionomers and indicates microphase separation of an ion-rich phase. As the temperature was raised, the ionomer peak weakened in intensity and broadened. The most significant decrease in the peak intensity occurred above ca. 190 °C, and the ionomer peak disappeared completely at ca. 245 °C, which indicates disappearance of the ionic domains. A similar decrease in intensity and broadening of the ionomer peak was previously observed for ZnSPS ionomers,[29] but in that case the peak never completely disappeared at temperature up to ca. 300 °C. The initial decrease of the intensity of the ionic peak at 190 °C for 8.7Zn-SSEBS coincides with the temperature at which a dynamic mechanical relaxation was observed in these same block copolymer ionomers[35] and in SPS ionomers[29] that was attributed to the onset of motion in the ionic aggregates.

The data in Figure 8 indicate that dissipation of the ionic structure begins at ca. 190 °C and is completed by 245 °C. The mesophase transition from an ellipsoidal to a lamellar block texture occurred in the different Zn-SSEBS ionomers between 200 and 250 °C, which suggests that the forces controlling the ionic microstructure and block microstructure are coupled. The extra forces acting on the ionic aggregates arising from the block copolymer structure lower the ionic dissociation temperature, and dissipation of the ionic aggregation is necessary before the block microdomains can reorganize.

SAXS curves for a compression-molded 12Cs-SSEBS over the temperature range of 110–300 °C are shown in Figure 9. In this case, the ionic microstructure persisted to at least 300 °C. The ionomer peak intensity first increased as the temperature was raised between 110 and 163 °C but then decreased above 163 °C. That behavior is reminiscent of the effect of temperature on the SAXS of Na-SPS ionomers.[29] The initial increase in the ionic peak may be due to thermal expansion and/or enhanced chain mobility above $(T_g)_{b\text{-CsSPS}}$ that allows more ionic groups to diffuse into the aggregates. The decrease in intensity above 163 °C indicates some dissociation of the ionic aggregates, but this is inconsequential compared with what occurs in the 8.7Zn-SSEBS(CM) ionomer.

The ionic structure in both M-SPS and M-SSEBS is more persistant in the two alkali salts, Na^+ and Cs^+, than in the Zn^{2+} salt, which indicates that the ion–dipole interactions of the latter are more temperature sensitive. As a result, sufficient dissociation of the ionic aggregates occurred in the Zn-SSEBS to allow reorganization of the block microstructure at elevated temperatures, while this was not observed for either alkali salt block copolymer ionomer. In addition, comparison of Figures 4 and 9 indicates that the ionic structure in the Na salt is more robust than that in the Cs salt. This is a consequence of the weakening of the ion–dipole interaction by the larger cation.

Effect of Sulfonation Level. T_d was relatively insensitive to the sulfonation level for the SSEBS block copolymer ionomers. When the sulfonation level was changed from 3 to 12 mol %, T_d only varied between 230 and 250 °C.

The development of ionic interactions within the *b*-SPS should increase the immiscibility of the two blocks of the copolymer. The energy required for a block

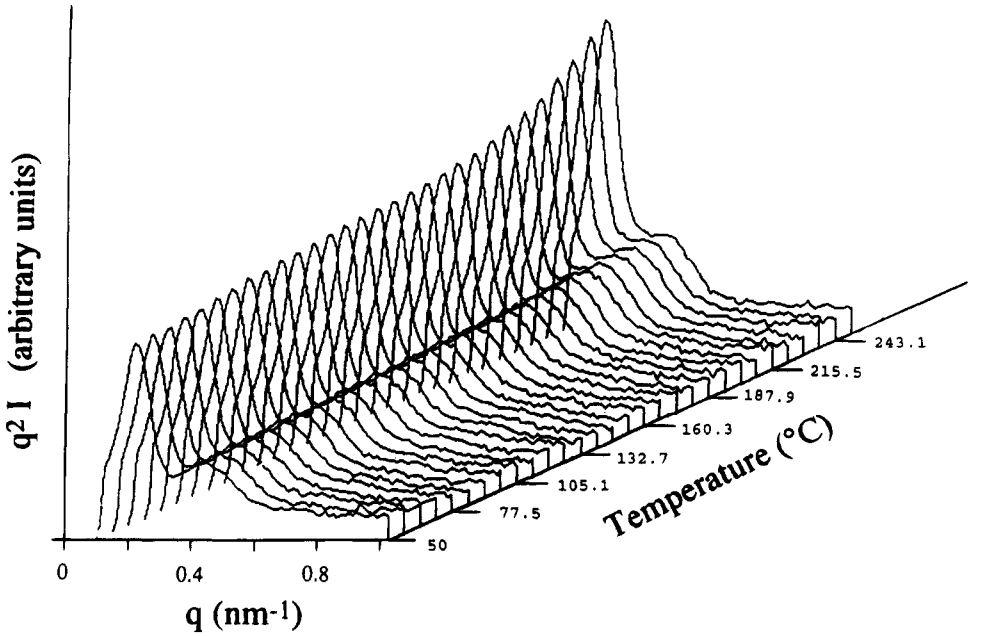

Figure 6. Temperature-resolved SAXS profiles for the block microstructure of solution-cast 12Zn-SSEBS obtained while heating from 50 to 250 °C.

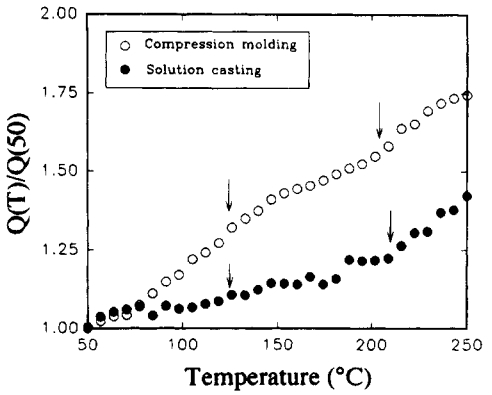

Figure 7. Experimental values of $Q(T)/Q(50)$ as a function of temperature for solution-cast (●) and compression-molded (○) 12Zn-SSEBS. The arrows denote the glass transition temperature of the *b*-SPS (lower temperature) and the mesophase–mesophase transition (upper temperature).

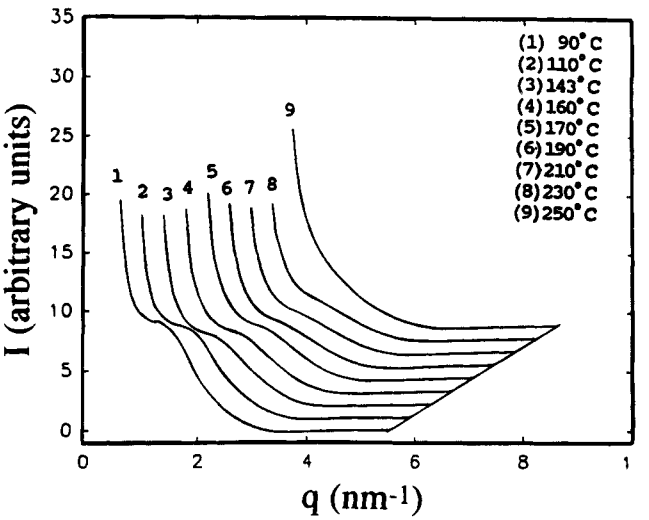

Figure 8. Temperature-resolved SAXS patterns for the ionic microstructure of compression-molded 8.7Zn-SSEBS obtained while heating from 90 to 250 °C.

phase transition is likely to increase as the concentration of ionic aggregates, i.e., physical cross-links, increases, and as a result, the block transition temperatures were expected to increase as the sulfonation level increased.

When the sulfonation level is relatively low, the temperature of the block ODT, T_{od}, may be lower than T_d. In that case, the ODT will occur as soon as the ionic aggregates dissociate. This is demonstrated by the SAXS data for 3Zn-SSEBS in Figure 10. The scattering maximum characteristic of the block microstructure persists only to T_d (ca. 230 °C). No mesophase–mesophase transition was observed for 3Zn-SSEBS, because of the coincidence of T_{od} and T_d.

For a higher sulfonation level, 8.7Zn-SSEBS, a mesophase–mesophase transition from an ellipsoidal to a lamellar microstructure occurred just above T_d at 240 °C (Figure 11). The mesophase transition is evident from the emergence of a second-order maximum in the scattering pattern at a q of twice that of the first-order maximum. Also apparent in Figure 11 is the reduction of the scattering intensity above T_d, which indicates that phase mixing also began after the ionic aggregates dissociated. It is normal for the extent of microphase mixing in a block copolymer to increase as the ODT is approached. T_{od}, however, was not observed for 8.7Zn-SSEBS; the data in Figure 11 indicate the block microphase persisted to at least 300 °C.

For the highest sulfonation level studied, 18Zn-SSEBS, the SAXS patterns below $(T_g)_{b\text{-ZnSPS}}$ and T_d exhibited a shoulder on the high-q side of the primary scattering peak (Figure 12). This result indicates that at low temperature the equilibrium block texture for the higher sulfonation level was already lamellar, though the texture was not well developed. The shoulder became more distinct above $(T_g)_{b\text{-ZnSPS}}$, but the most significant changes in the scattering pattern occurred above T_d (ca. 250 °C). In addition to the clear resolution of a second maximum above T_d, the scattering intensity increased. This is in marked contrast to the decrease that was observed above T_d for 8.7Zn-SSEBS. The increase of the scattering intensity indicates that additional microphase separation of the block morphology occurred, rather than phase mixing. These results may

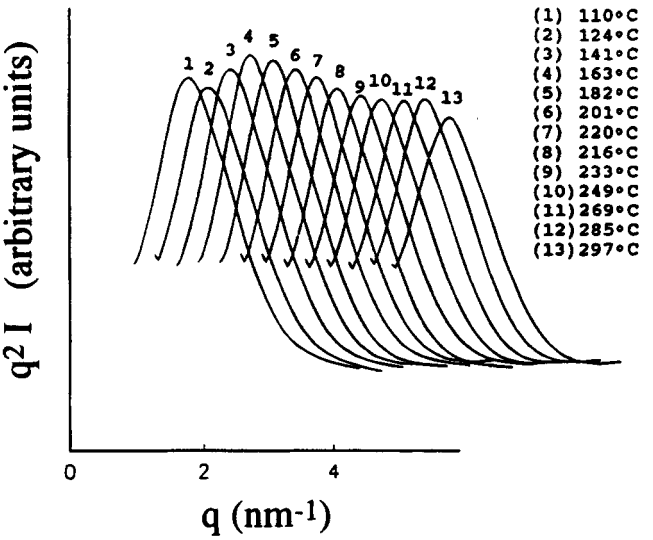

Figure 9. Temperature-resolved SAXS patterns for the block microstructure of compression-molded 12Cs-SSEBS obtained while heating from 110 to 300 °C.

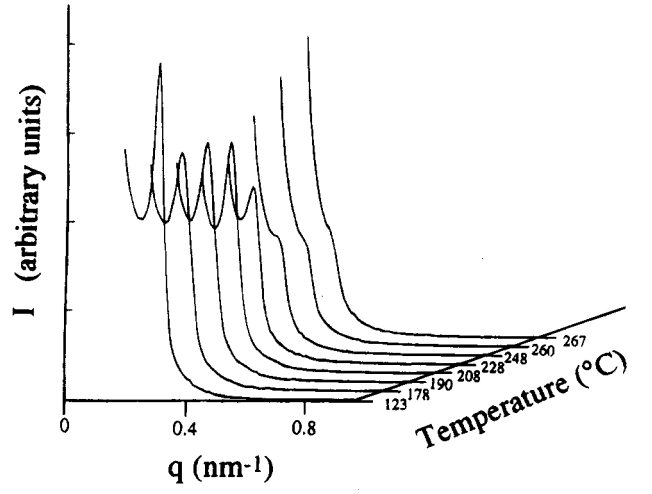

Figure 10. Temperature-resolved SAXS patterns for the block microstructure of compression-molded 3Zn-SSEBS obtained while heating from 123 to 267 °C.

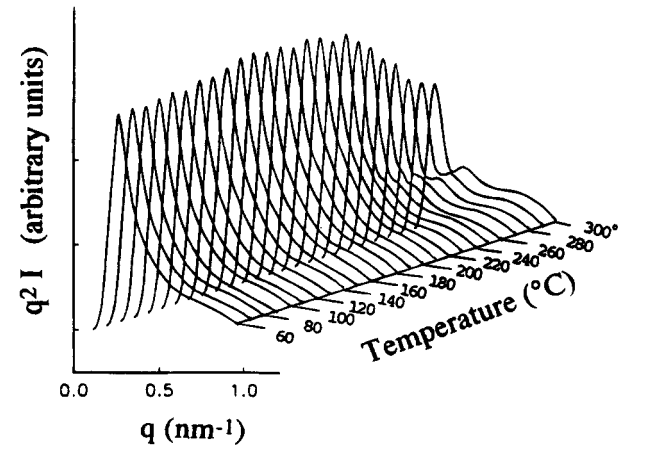

Figure 11. Temperature-resolved SAXS patterns for the block microstructure of compression-molded 8.7Zn-SSEBS obtained while heating from 60 to 300 °C.

be explained by the high melt viscosity that develops due to ionic association. The high viscosity impedes facile formation of the block microstructure during compression molding. Clearly, no block phase transitions, phase mixing, or additional microphase separation can occur until the ionic aggregates dissociate, i.e., until the physical cross-link network formed from ionic associations becomes sufficiently weak to allow reorganization of the block chains. The impediment to chain motion resulting from the ionic interactions becomes more severe as the ionic group concentration increases.

Figure 13 shows that when the heated 18Zn-SSEBS sample was cooled back to room temperature, no further changes in the scattering pattern were observed. This result further confirms that the changes in the scattering shown in Figure 12 arose from the development of a nonequilibrium morphology during compression molding and not from a thermodynamic transition.

Conclusions

M-SSEBS block copolymer ionomers exhibit two separate microphase structures: a block texture and ionic aggregates within the polystyrene-rich domains. An ionic aggregate dissociation transition was observed for the free acid derivative and the Zn salts. That finding represents the first time a thermally-induced order–disorder transition has been experimentally observed for an ionomer. In some cases, a mesophase to mesophase transition from an ellipsoidal to a lamellar block microstructure and/or an order–disorder transition of the block microphase separation were observed above the ionic aggregate dissociation temperature, T_d. T_d was relatively insensitive to the sulfonation level but was a function of the cation used. For H-SSEBS, $T_d \sim$ 175 °C, and for Zn-SSEBS, $T_d \sim$ 235–250 °C. The ionic aggregates in the alkali-metal-neutralized ionomers were thermally stable to at least 300 °C, and no microphase transitions were observed for those ionomers.

Thermally-induced transitions of the block microstructure were strongly dependent on the sulfonation level of the ionomer. At low sulfonation levels (3 mol % of the styrene blocks), the temperature of the order–disorder transition, T_{od}, coincided with T_d, and no mesophase–mesophase transition was observed. For an intermediate sulfonation level (8.7 mol %), a mesophase transition from an ellipsoidal to a lamellar microstructure and partial mixing of the block microphases occurred above T_d. In that case, $T_{od} > T_d$ and the block copolymer ODT was not observed. For the highest sulfonation level studied (18 mol %), a highly ordered microstructure was exceedingly difficult to obtain by compression molding. 18Zn-SSEBS had a poorly developed lamellar microstructure at room temperature, which became more organized by thermal annealing as motion of the block chains was allowed, first above the T_g of the sulfonated polystyrene block and, again, above T_d. The latter transition was clearly more important with regard to chain mobility and reorganization of the microstructure. Moreover, for 18Zn-SSEBS $T_{od} \gg T_d$ and no evidence of the order–disorder transition was observed below the degradation temperature of the polymer.

Although the results described in this paper are not inclusive, it is clear that the introduction of a strong associative interaction within one of the blocks of a block copolymer has a considerable influence on the thermodynamic transitions and the microstructure texture of the block copolymer. Similarly, confining an ionomer to the restricted geometry of a block copolymer perturbs the thermodynamics of its microphase separation. In this case, a suppression of the aggregate dissociation temperature was observed.

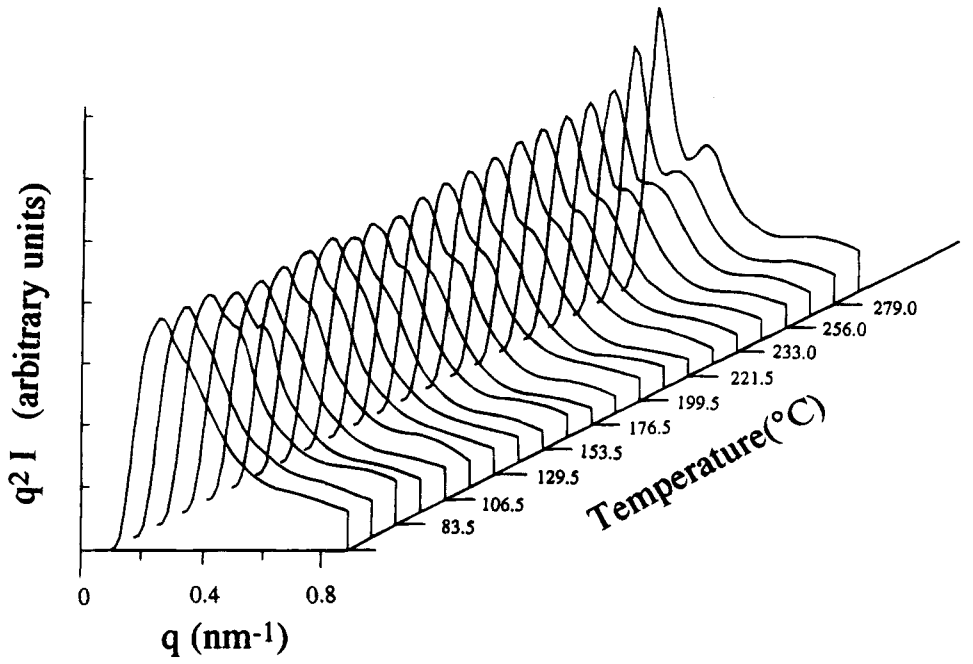

Figure 12. Temperature-resolved SAXS patterns for the block microstructure of compression-molded 18Zn-SSEBS obtained while heating from 60 to 300 °C.

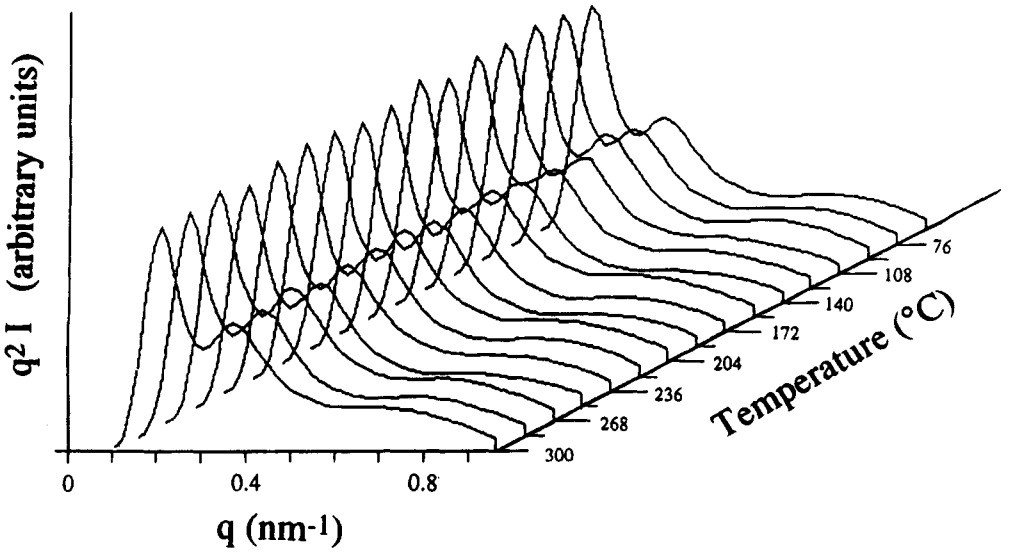

Figure 13. Temperature-resolved SAXS patterns for the block microstructure of compression-molded 18Zn-SSEBS obtained while cooling from 300 to 60 °C.

We are not aware of any other experimental or theoretical treatments of the temperature dependence of the microstructure of block copolymer ionomers, though a study by Russell et al.[41] on the microstructure of block copolymers formed via ionic interactions between telechelic oligomers is particularly notable with respect to the current paper. In that paper, the authors proposed phase diagrams that include the ODT of the block copolymer, the dissociation temperature of the ionic interactions, and an upper critical solution temperature of the blend. They discuss the interdependence of the three transitions and note that macrophase mixing of the oligomers cannot occur until T_d (T_i in their paper) is exceeded. Although Russell et al. present no experimental confirmation of their proposed phase diagrams, the data presented here for the block copolymer ionomers are in many ways consistent with the ideas contained in ref 41.

Theories of block copolymers[11,12] predict that the microphase texture may change reversibly with temperature. This has been experimentally confirmed in a recent report by Hajduk et al.[19] Sakurai et al.[17] also reported a thermally-induced morphology transition for a block copolymer, but in that case, the transition was a consequence of freezing-in a nonequilibrium microstructure during sample preparation and, therefore, the transition was irreversible. Although it remains to be confirmed that the mesophase–mesophase transition reported here truly represents a reversible, thermodynamic event, the samples were compression-molded, which makes it unlikely that they possessed nonequilibrium textures as achieved by Sakurai et al.[17] when they cast a block copolymer film from a selective solvent.

Our results suggest that the temperature sensitivity of intermolecular interactions, which probably affect the segregation power of the block copolymer, may perturb the thermodynamics of the block copolymer such that the equilibrium textures are affected and mesophase transitions become more pronounced. This may be a useful result in terms of controlling the morphology of

block copolymers, at least in the case of styrenic block copolymers where the sulfonation chemistry is especially facile. Currently, our research is directed at a more complete understanding of these phenomena. We have prepared a series of di- and triblock copolymer ionomers where both the block composition and the sulfonation level are varied. Rheological and SAXS studies will be reported in a future paper.

Acknowledgment. We gratefully acknowledge support of this research by the Office of Naval Research (Grant N00014-91-J-1565). We also thank Dr. Carl Willis of Shell Development Co. for providing the starting SEBS block copolymer and Dr. Tom Russell and Prof. Jeff Koberstein for their help with the SAXS experiments at SSRL. Access to the SUNY Beamline at Brookhaven National Laboratory, which is supported by the Department of Energy, was kindly provided by Prof. Benjamin Chu.

References and Notes

(1) Sperling, L. H., Ed. *Recent Advances in Polymer Blends, Grafts and Blocks*; Plenum: New York, 1974.
(2) Goodman, I., Ed. *Developments in Block Copolymers*; Elsevier: New York, 1982; Vol. 1.
(3) Eisenberg, A.; King, M. *Ion-Containing Polymers*; Academic Press: New York, 1977.
(4) Pineri, M., Eisenberg, A., Eds. *Structure and Properties of Ionomers*; D. Reidel Publishing Co.: Dordrecht, Holland, 1987.
(5) Meier, D. J. *J. Polym. Sci.* **1969**, *C26*, 81.
(6) Meier, D. J. In *Block and Graft Copolymers*; Burke, J. J., Weiss, V., Eds.; Syracuse University Press: Syracuse, NY, 1973.
(7) Helfand, E. *Macromolecules* **1975**, *8*, 552.
(8) Helfand, E.; Wasserman, Z. R. *Macromolecules* **1976**, *9*, 879.
(9) Helfand, E.; Wasserman, Z. R. *Macromolecules* **1978**, *11*, 960.
(10) Helfand, E.; Wasserman, Z. R. *Macromolecules* **1980**, *13*, 994.
(11) Leibler, L. *Macromolecules* **1980**, *13*, 1602.
(12) Fredrickson, G. H.; Helfand, E. *J. Chem. Phys.* **1987**, *87*, 697.
(13) Bates, F. S. *Macromolecules* **1984**, *17*, 2607.
(14) Leung, L. M.; Koberstein, J. T. *Macromolecules* **1986**, *19*, 706.
(15) Roe, R. J.; Fishkis, M.; Chang, C. J. *Macromolecules* **1981**, *14*, 1091.
(16) Owens, J. N.; Gancarz, I. S.; Koberstein, J. T.; Russell, T. P. *Macromolecules* **1989**, *22*, 3380.
(17) Sakurai, S.; Momii, T.; Taie, K.; Shibayama, M.; Nomura, S.; Hashimoto, T. *Macromolecules* **1993**, *26*, 485.
(18) Lu, X.; Steckle, W. P., Jr.; Weiss, R. A. *Proc. An. Tech. Conf., Soc. Plast. Eng.* **1993**.
(19) Hajkuk, D. A.; Gruner, S. M.; Rangarajan, P.; Register, R. A.; Fetters, L. J.; Honeker, C.; Albalak, R. J.; Thomas, E. L. *Macromolecules* **1994**, *27*, 490.
(20) MacKnight, W.; Earnest, T. *J. Polym. Sci., Macromol. Rev.* **1981**, *16*, 41.
(21) Wilson, A. D., Prosser, H. J., Eds. *Developments in Ionic Polymers-1&2*; Applied Science Publishers: New York, 1983.
(22) Fitzgerald, J. J.; Weiss, R. A. *J. Macromol. Sci., Rev.* **1988**, *C28*, 99.
(23) Mauritz, K. A. *J. Macromol. Sci., Rev.* **1988**, *C28*, 65.
(24) MacKnight, W. J.; Taggart, W. P.; Stein, R. S. *J. Polym. Sci., Polym. Symp.* **1974**, *45*, 113.
(25) Fujimura, M.; Hashimoto, T.; Kawai, H. *Macromolecules* **1982**, *15*, 136.
(26) Yarusso, D. J.; Cooper, S. L. *Macromolecules* **1983**, *16*, 1871.
(27) Eisenberg, A. *Macromolecules* **1970**, *3*, 147.
(28) Yarusso, D. J.; Cooper, S. L. *Polymer.* **1985**, *26*, 371.
(29) Weiss, R. A.; Lefelar, J. A. *Polymer.* **1986**, *27*, 3.
(30) Williams, C. E.; Russell, T. P.; Jérôme, R.; Horrion, J. *Macromolecules* **1986**, *19*, 2877.
(31) Gauthier, S.; Eisenberg, A. *Macromolecules* **1987**, *20*, 760.
(32) Long, T. E.; Allen, R. D.; McGrath, J. E. In *Chemical Reactions on Polymer*; Benham, J. L.; Kinstle, J., Eds.; American Chemical Society: Washington DC, 1988.
(33) Weiss, R. A.; Sen, A.; Pottick, L. A.; Willis, C. L. *Polym. Commun.* **1990**, *31*, 220.
(34) Venkateshwaran, L. N.; York, G. A.; DePorter, C. D.; McGrath, J. E.; Wilkes, G. L. *Polymer* **1992**, *33*, 2277.
(35) Weiss, R. A.; Sen, A.; Pottick, L. A.; Willis, C. L. *Polymer* **1991**, *32*, 2785.
(36) Lu, X.; Steckle, W. P., Jr.; Weiss, R. A. *Macromolecules* **1993**, *26*, 5876.
(37) Lu, X.; Steckle, W. P., Jr.; Weiss, R. A. *Macromolecules* **1993**, *26*, 6525.
(38) Stephenson, G. B. Ph.D. Dissertation, Stanford University, 1982.
(39) Chu, B.; Wu, D. Q.; Wu, C. *Rev. Sci. Instrum.* **1987**, *58*, 1158.
(40) Porod, G. *Kolloid Z.* **1951**, *124*, 83; **1952**, *125*, 51.
(41) Russell, T. P.; Jérôme, R.; Charlier, P.; Foucart, M. *Macromolecules* **1988**, *21*, 1709.

MA9460091